

(This is a sample cover image for this issue. The actual cover is not yet available at this time.)

This article appeared in a journal published by Elsevier. The attached copy is furnished to the author for internal non-commercial research and education use, including for instruction at the authors institution and sharing with colleagues.

Other uses, including reproduction and distribution, or selling or licensing copies, or posting to personal, institutional or third party websites are prohibited.

In most cases authors are permitted to post their version of the article (e.g. in Word or Tex form) to their personal website or institutional repository. Authors requiring further information regarding Elsevier's archiving and manuscript policies are encouraged to visit:

<http://www.elsevier.com/copyright>



Contents lists available at ScienceDirect

## Dyes and Pigments

journal homepage: [www.elsevier.com/locate/dyepig](http://www.elsevier.com/locate/dyepig)

# A comparative study of a novel lipophilic phthalocyanine incorporated into nanoemulsion formulations: Photophysics, size, solubility and thermodynamic stability

María C. García Vior<sup>a,\*</sup>, Ezequiel Monteagudo<sup>b</sup>, Lelia E. Dicio<sup>c</sup>, Josefina Awruch<sup>a,\*</sup>

<sup>a</sup> Departamento de Química Orgánica, Facultad de Farmacia y Bioquímica, Universidad de Buenos Aires, Junín 956, 1113 Buenos Aires, Argentina

<sup>b</sup> Departamento de Tecnología Farmacéutica, Facultad de Farmacia y Bioquímica, Universidad de Buenos Aires, Junín 956, 1113 Buenos Aires, Argentina

<sup>c</sup> INQUIMAE, Departamento de Química Inorgánica, Analítica y Química Física, Facultad de Ciencias Exactas y Naturales, Universidad de Buenos Aires, Ciudad Universitaria, Pabellón II, 1428 Buenos Aires, Argentina

## ARTICLE INFO

## Article history:

Received 5 January 2011

Received in revised form

4 March 2011

Accepted 7 March 2011

Available online 16 March 2011

## Keywords:

Photodynamic therapy

Zinc(II) phthalocyanines

Nanoemulsions

Thermodynamic stability

Solubility

Singlet oxygen

## ABSTRACT

Lipophilic tetrakis-(1-adamantylsulfanyl)phthalocyaninatozinc(II) was incorporated into two different nanoemulsion formulations with the former emulsion containing isopropyl myristate and Tween 80® and the latter glycerol monocaprylocaprate and Tween 80®. A two- to three-fold increase in water solubility was observed for the zinc phthalocyanine when incorporated into the nanoemulsions in comparison with that observed for water–DMSO (98:2). Morphological evaluation confirmed the formation of thermodynamically stable nanoemulsions in the nanosize range. The zinc phthalocyanine incorporated into the nanoemulsions was photo-stable over the irradiation times studied and both formulations displayed excellent singlet oxygen generation ability with high values of quantum yield of singlet oxygen production of up to 0.58. In addition, the viscosity of the nanoemulsions ranged from 30.2 to 323.9 cP. The foregoing formulations are considered to be strong candidates for parenteral administration of the zinc phthalocyanine in photodynamic therapy clinical trials.

© 2011 Elsevier Ltd. All rights reserved.

## 1. Introduction

Photodynamic therapy (PDT) is an anti-tumor treatment procedure based on the ability of the photosensitizer to accumulate selectively in tumor tissues; cell damage or cell death can be induced by light irradiation of the tumoral tissues at the appropriate wavelength, with a suitable photosensitizer and in the presence of molecular oxygen [1].

Phthalocyanines are very promising photosensitizers, but most of them are soluble only in organic solvents, which, in most cases, are not allowed in pharmaceutical formulations [2–4]. A significant challenge that needs to be overcome in most treatments is the hydrophobic nature of phthalocyanines, which severely hampers intravenous administration through the bloodstream. Thus, it is necessary to develop suitable delivery systems such as oil-dispersions, liposomes, polymeric particles (nanoparticles and microparticles) or hydrophilic polymer-photosensitizer conjugates [5–9].

The ideal drug delivery system should enable the selective accumulation of the photosensitizer within the diseased tissue and the delivery of therapeutic concentrations of photosensitizer to the target site with little or no uptake by non-target cells. The carrier must also be able to incorporate the photosensitizer without loss or alteration of its activity.

One of the most promising technologies is the nanoemulsion drug delivery system, which is being applied to enhance the solubility and bioavailability of hydrophobic drugs. Nanoemulsions are transparent dispersions of oil and water stabilized by an interfacial film of surfactant molecules that have a droplet size smaller than 100 nm. Nanoemulsions have higher solubilization capacity than simple micellar solutions and their thermodynamic stability offers advantages over unstable dispersions, such as emulsions and dispersions, because they can be manufactured with little energy input and have a long shelf life. The nanosized droplets that lead to an enormous increase in the interfacial areas associated with nanoemulsions would influence the transport properties of the drug, an important factor in sustained and targeted drug delivery [10,11].

The great interest in the development of the above mentioned phthalocyanine delivery systems has led us to investigate the

\* Corresponding authors. Tel.: +54 11 49648252; fax: +54 11 45083645.  
E-mail address: [jawruch@ffyb.uba.ar](mailto:jawruch@ffyb.uba.ar) (J. Awruch).

spectroscopic and photophysical properties, as well as the size, solubility and thermodynamic stability of the lipophilic tetrakis-(1-adamantylsulfanyl)phthalocyaninatozinc(II) incorporated into two different nanoemulsion formulations.

## 2. Materials and methods

### 2.1. Chemical and reagents

2,9(10),16(17),23(24)-tetrakis-(1-adamantylsulfanyl)phthalocyaninatozinc(II) (ZnPc) [12] (Fig. 1) and tetra-*t*-butyl phthalocyaninatozinc(II) [13] were synthesized in our laboratory. Isopropyl myristate (IPM) was purchased from Merck (Germany). Polyoxyethylene sorbitan mono oleic acid (Tween 80<sup>®</sup>) was obtained from Fisher Chemicals (New Jersey, USA). Glycerol monocaprylocaprate (Capmul MCM-L<sup>®</sup>) was purchased from Abitec (Columbus, USA). Imidazole BioUltra and Methylene Blue Hydrate (MB) were obtained from Fluka (Sigma–Aldrich, India). *N,N*-Diethyl-4-nitrosoaniline 97%, dimethylsulfoxide (DMSO) and tetrahydrofuran (THF) spectrophotometric grade were purchased from Sigma–Aldrich (Steinheim, Germany). All chemicals were of reagent grade and used without further purification. Distilled water treated in a Milli-Q system (Millipore) was used.

### 2.2. Instrumentation

Electronic absorption spectra were determined with a Shimadzu UV-3101 PC spectrophotometer. Fluorescence spectra were monitored with a QuantaMaster Model QM-1 PTI spectrofluorometer. Viscosity was determined using a Brookfield DV III ultra V6.0 RV cone and plate rheometer using a small sample adapter spindle N° 18. Conductivity measurements were performed using an Accumet Research ar20. Mixing was performed using a magnetic mixing, IKA. Droplet size measurements were evaluated with dynamic light scattering (DLS) using a Malvern Nanosizer/Zetasizer<sup>®</sup> nano-ZS ZEN 3600 (Malvern Instruments, UK), provided with a 4 mW He–Ne (633 nm). Transmission electron microscopy (TEM)

nanoemulsion images were obtained by means of an EM 301 Phillips operating at 65 kV.

### 2.3. Preparation of ZnPc-loaded nanoemulsions

Nanoemulsions were prepared according to the spontaneous emulsification method [14]. The selected formulations for drug incorporation were NE1 (IPM 4%, Tween 80<sup>®</sup> 25%) and NE2 (Capmul MCM-L<sup>®</sup> 4%, Tween 80<sup>®</sup> 25%). A preliminary mix of surfactant, lipid and ZnPc was prepared weighing an adequate amount of each one. The preparation was then mixed using a magnetic stirrer until a homogeneous sample was obtained. While mixing, the sample was heated to 40 °C in order to improve the homogenization. Water was then added at the same temperature and stirring continued up to homogeneity. Samples were stored at room temperature and carefully protected from ambient light. Blank formulations were also prepared.

### 2.4. Characterization of nanoemulsions

#### 2.4.1. Transmission electron microscopy

The morphology of nanoemulsions was studied using TEM. In order to perform the TEM observations, the concentrated nanoemulsions were first diluted in water (1:100), a sample drop was placed onto a grid covered with Formvar film and the excess was drawn off with a filter paper. Samples were subsequently stained with uranyl acetate solution for 30 s. Samples were finally dried in a closed container with silicagel and analyzed. The droplet diameter was estimated using a calibrated scale.

#### 2.4.2. Droplet size measurements

Droplet size measurements were evaluated with DLS. Samples were not diluted before measurements and assays were performed at 25 °C. Experiments were carried out without photosensitizer to prevent fluorescence interference in the light scattering signals.

#### 2.4.3. Viscosity determination

The viscosity of the formulations (10 mL) was determined without dilution at 25 ± 0.5 °C.

### 2.5. Solubility studies

#### 2.5.1. Determination of ZnPc solubility in DMSO and water–DMSO (98:2)

The solubility of ZnPc in pure DMSO and water–DMSO (98:2) was studied by UV spectrophotometry; 2% DMSO is the maximum concentration usually tolerated by cell monolayers *in vitro*. A stock solution of 0.16 mM ZnPc in DMSO was prepared and confirmed using the absorbance at 685 nm ( $\epsilon_{\text{ZnPc}} = 1.0 \times 10^5 \text{ M}^{-1} \text{ cm}^{-1}$ ) and subsequently diluted to obtain 2.38, 1.59, 0.80, 0.32, 0.16  $\mu\text{M}$  solutions. The absorbance was measured at the corresponding  $\lambda_{\text{max}}$  at 23 °C. Concentrations were calculated by interpolating the absorbance of each sample in a calibration curve, covering the range between 0.16 and 2.38  $\mu\text{M}$  (correlation factors were 0.9974–0.9984). Solvents were used as blanks. Experiments were carried out in duplicate and concentrations are expressed in  $\mu\text{M}$ . The intrinsic solubility ( $S_0$ ) of ZnPc in DMSO and aqueous medium was defined as the highest concentration measured for any of the solutions on day 30 [15].

#### 2.5.2. Determination of ZnPc solubility in nanoemulsions

The solubility of ZnPc in nanoemulsions NE1 and NE2 was studied by UV spectrophotometry. Stock solutions of 0.1 mM ZnPc in NE1 and NE2 were prepared and subsequently diluted to obtain 2.44, 1.64, 0.83, 0.33, 0.17  $\mu\text{M}$  solutions. The absorbance was

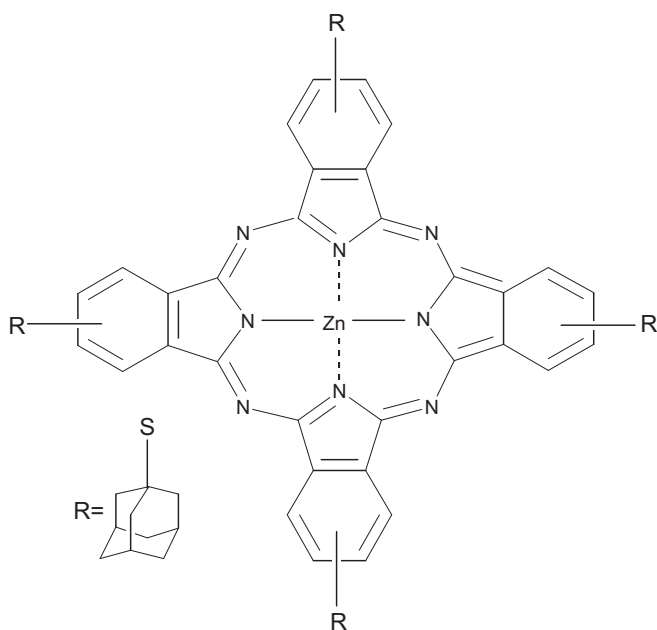


Fig. 1. Chemical structure of phthalocyanines (ZnPc).

measured at the corresponding  $\lambda_{\max}$  at 23 °C. Concentrations were calculated by interpolating the absorbance of each sample in a calibration curve covering the range between 0.17 and 2.44  $\mu\text{M}$  (correlation factors were 0.9981–0.9992).

Solvents were used as blanks. Experiments were carried out in duplicate and concentrations are expressed in  $\mu\text{M}$ .

## 2.6. Photophysical parameters

### 2.6.1. Spectroscopic studies

Absorption and emission spectra were recorded at different concentrations using a  $10 \times 10$  mm quartz cuvette. All experiments were performed at room temperature.

Emission spectra of ZnPc were collected at an excitation wavelength of 610 nm (Q-band) and recorded between 630 and 800 nm.

The emission and absorption spectra of the ZnPc-loaded nanoemulsions were corrected for light scattering by subtracting the spectra from empty nanoemulsions.

Spectroscopic experiments were recorded at concentrations in a range of 0.6  $\mu\text{M}$ –4  $\mu\text{M}$  for ZnPc.

### 2.6.2. Fluorescence quantum yields

Fluorescence quantum yields ( $\Phi_F$ ) were determined by comparison with those of tetra-*t*-butyl phthalocyaninatozinc(II) ( $\Phi_F = 0.30$  in toluene) [13] as a reference at  $\lambda_{\text{exc}} = 610$  nm. Calculation were performed by Equation (1),

$$\Phi_F^S = \Phi_F^R \frac{I^S (1 - 10^{-A^R})}{I^R (1 - 10^{-A^S})} \left( \frac{n^S}{n^R} \right)^2 \quad (1)$$

where *R* and *S* superscripts refer to the reference and the sample respectively; *I* is the integrated area under the emission spectrum; *A* is the absorbance of solutions at the excitation wavelength and  $(n^S/n^R)^2$  stands for the refractive index correction.

### 2.6.3. Quantum yield of singlet oxygen production

The quantum yield of singlet oxygen generation rates ( $\Phi_\Delta$ ) was calculated by means of standard chemical monitor bleaching rates [16]. Imidazole (8 mM) and N,N-diethyl-4-nitrosoaniline (40–50  $\mu\text{M}$ ) in water was used for ZnPc-loaded nanoemulsions as a singlet oxygen chemical quencher [17]. The bleaching of nitrosoaniline was followed spectrophotometrically at 440 nm as a function of time. Polychromatic irradiation was performed using a projector lamp (Philips 7748SEHJ, 24 V–250 W), and a cut-off filter at 610 nm (Schott, RG 610) and a water filter were used to prevent infrared radiation. Nanoemulsion samples of ZnPc and references (MB:  $\Phi_\Delta = 0.56$  in water) [16] were irradiated within the same wavelength interval  $\lambda_1$ – $\lambda_2$ , and  $\Phi_\Delta$  was calculated according to Equation (2),

$$\Phi_\Delta^S = \Phi_\Delta^R \frac{r^S \int_{\lambda_1}^{\lambda_2} I_0(\lambda) (1 - 10^{-A^R(\lambda)}) d\lambda}{r^R \int_{\lambda_1}^{\lambda_2} I_0(\lambda) (1 - 10^{-A^S(\lambda)}) d\lambda} \quad (2)$$

where *r* is the singlet oxygen photogeneration rate and the superscripts *S* and *R* stand for the sample and reference respectively, *A* is the absorbance at the irradiation wavelength and  $I_0(\lambda)$  is the incident spectral photon flow ( $\text{mol s}^{-1} \text{nm}^{-1}$ ). When the irradiation wavelength range is narrow, the incident intensity varies smoothly with wavelength and the sample and reference have overlapping

spectra,  $I_0$  can be approximated by a constant value which may be drawn out of the integrals and canceled.

## 2.7. Photo-oxidative stability

The photo-stability of phthalocyanines incorporated into NE1 and NE2 was determined by the decay of the Q-band intensity after exposure to red light [18]. The fluence rate was adjusted to 20  $\text{mW cm}^{-2}$ . Measurements were performed under air in water. Photodegradation rate constants *k* were calculated by Equation (3),

$$\ln \frac{A_0}{A_t} = k \cdot t \quad (3)$$

where *t*,  $A_0$ ,  $A_t$  are the irradiation time, absorbance at *t* = 0, absorbance at different times, respectively.

## 2.8. Thermodynamic stability studies

To overcome the problem of metastable formulation, thermodynamic stability tests were performed [19]. Six cycles between refrigerator temperature (4 °C) and 45 °C with storage at each temperature of not less than 48 h were studied. The formulations, which were stable at these temperatures, were subjected to a centrifugation test. Passed formulations were centrifuged at 3500 rpm for 30 min. The formulations that did not show any phase separation were used for the freeze–thaw cycle test. Three freeze–thaw cycles between –21 °C and 25 °C with storage at each temperature for not less than 48 h were carried out for the formulations.

Samples that survived the thermodynamic stability tests were selected for further studies.

## 3. Results and discussions

The oils chosen in the present study are widely used as oil phases for nanoemulsion formulations. Several works have tested different administration routes for these oils and shown that they all are physiologically tolerable oils [20,21]. The selection of the oily phase of the nanoemulsion is very important because the solubility of the drug in the formulation is critically dependant on this factor [22,23]. From this point of view, IPM and Capmul MCM-I<sup>®</sup> were selected for a forthcoming screening due to their high ZnPc solubilization capacity.

### 3.1. Characterization of the nanoemulsions

The nanoemulsions obtained presented a homogeneous aspect without aggregates or phase separation. Fig. 2 depicts electron micrographs of formulation samples, which appear as spherical-shaped vesicles. The nanoemulsions presented a uniform diameter of 5–10 nm for NE1 and of 10–20 nm for NE2, which is consistent with previous reports [19,24].

Regarding droplet size measurements, it should be noted that samples showed two droplet size populations (Fig. 3), the most abundant of which was considered as the main one. As shown in Fig. 3, the mean size diameter for formulations NE1 and NE2 was around 5 nm, whereas the secondary population was around 13–14 nm. The main droplet size of both formulations is, according to bibliography, in the range of a nanoemulsion. It is well known that the droplet size is one of the most important characteristics of a nanoemulsion because it affects its stability [25] and later *in vivo* behavior [26]. The polydispersity for the size distribution of formulations NE1 and NE2 was in the range of 0.399–0.400.



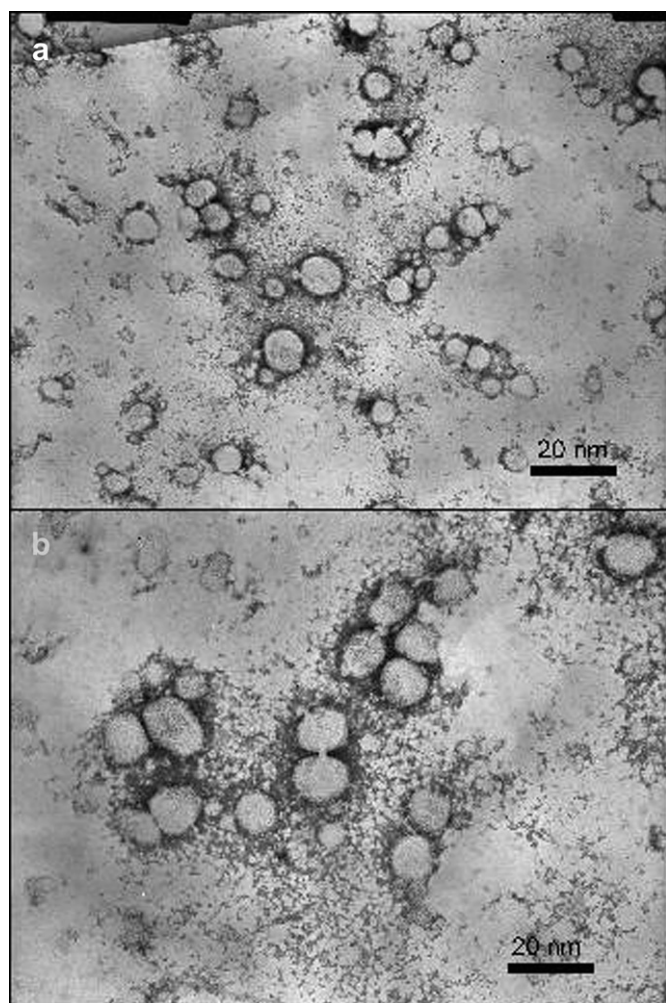


Fig. 2. Transmission electron microscopy images of NE1 (a) and NE2 (b).

As shown in Table 1, the conductivity values corresponded to that of an oil in water nanoemulsion where the continuous phase is water [27,28].

The viscosity of the nanoemulsion formulations was very low, showing the NE1 formulation a lower value than NE2 (Table 1). It is well known that one of the nanoemulsion characteristics is low

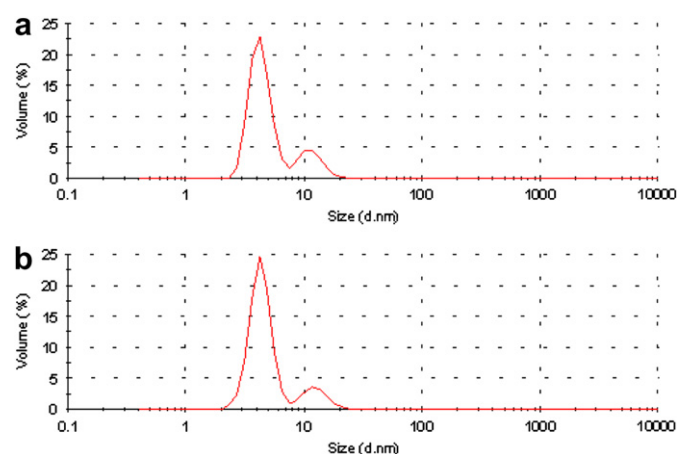


Fig. 3. Particle size distribution of NE1 (a) and NE2 (b).

Table 1

Composition and physical parameters of nanoemulsions.

Nanoemulsion	Composition	Conductivity $\mu\text{S cm}^{-1}$	Viscosity cP
NE1	IPM 4% Tween 80® 25%	166	30.2
NE2	Capmul MCM-L 4% Tween 80® 25%	251	323.9

viscosity [11]. Moreover, viscosity values discard the fact that formulas are liquid crystals instead of nanoemulsions.

### 3.2. Solubility studies

The solubility of ZnPc was investigated in pure DMSO, water–DMSO (98:2), NE1, and NE2. The former is a good solvent for ZnPc whereas the second one is similar to that used in culture medium. Solutions with concentrations between 0.16 and 2.44  $\mu\text{M}$  were prepared and the absorption was monitored over time. This concentration range is in agreement with the well-established range of LD<sub>50</sub> for most zinc (II) phthalocyanines [29].

To evaluate the solubility of ZnPc, the concentrations were monitored over one month, (Fig. 4). The intrinsic solubility in DMSO, water–DMSO (98:2), NE1, and NE2 was 1.77  $\mu\text{M}$ , 0.17  $\mu\text{M}$ , 0.37  $\mu\text{M}$  and 0.56  $\mu\text{M}$ , respectively. A two- to three-fold increase in water solubility was observed for the ZnPc incorporated into NE1 and NE2 nanoemulsions in comparison with that observed for water–DMSO (98:2).

### 3.3. Photophysical parameters

#### 3.3.1. Spectroscopic studies

Absorption and emission spectra of free ZnPc and ZnPc incorporated into nanoemulsions were performed according to conventional methods for homogeneous media. Fig. 5 shows the incorporation of ZnPc in homogeneous media (THF) and into nanoemulsions. The absorption spectra of ZnPc incorporated into NE1 and NE2 in the range of 500–800 nm range were similar to those previously reported for other zinc(II) phthalocyanines in homogeneous media [2,13,30]. The spectra in THF and into nanoemulsions recorded at [ZnPc] = 0.6  $\mu\text{M}$ –4  $\mu\text{M}$  showed a linear behavior (inset Fig. 5), obeying the Beer–Lambert equation, as only monomers are present in the solution. The absorption spectra of ZnPc incorporated into NE2 showed no relevant modifications in shape and wavelength and the only difference was the magnitude of the absorption coefficient (Table 2). A different spectral behavior was observed for ZnPc-loaded nanoemulsion NE1, where no relevant modification in wavelength was detected but some differences in shape were observed, probably due to an increase in the transition properties of the vibrational bands 0–1 0–2 caused by the confinement of ZnPc in the nanoemulsion and not to the formation of aggregates since the bands do not correspond to dimer species.

The fluorescence emission spectra of the ZnPc incorporated into nanoemulsions are shown in Fig. 5. For both formulations, neither significant wavelength shifts nor relevant modifications in spectral shapes were observed with an increase in dye concentration. In view of these results, fluorescence can be attributed to monomers alone.

#### 3.3.2. Fluorescence quantum yields

$\Phi_F$  values in homogeneous and microheterogeneous media are listed in Table 2. The ZnPc incorporated into nanoemulsions presented lower values of  $\Phi_F$  in comparison with homogeneous media. The differences observed in the values in both media (THF and nanoemulsions) may be due to the influence of the environment

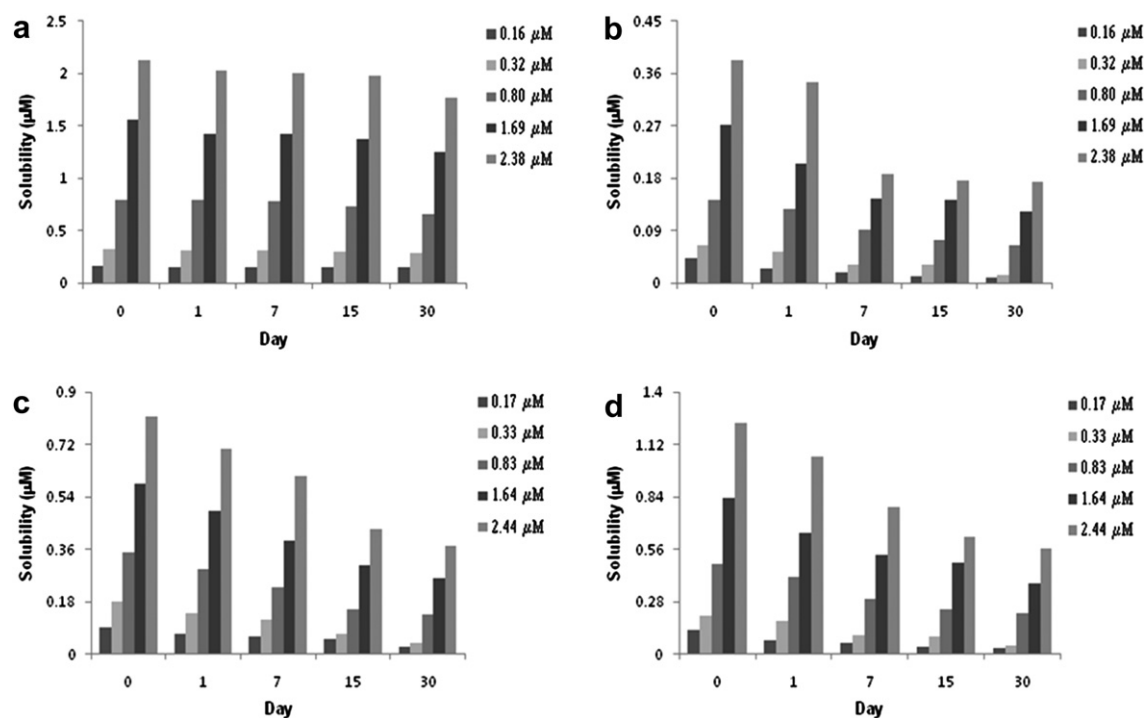


Fig. 4. Solubility of ZnPc in DMSO (a), Water–DMSO (98:2) (b), NE1 (c), and NE2 (d), over one month.

contribution with a non-radiative process of electronic-to-vibrational energy transfer [2,3,31]. The above mentioned results are similar to those described elsewhere [32].

### 3.3.3. Singlet molecular oxygen quantum yields

Sample absorbances were kept as low as possible to prevent aggregation, though sufficient to obtain measurable values of quantum yield of singlet molecular oxygen. As shown in Table 2, the  $\Phi_{\Delta}$  values of the ZnPc incorporated into nanoemulsions were lower than those observed in homogeneous media. However, these values were higher than those obtained for other phthalocyanines incorporated into liposomes [2,32].

### 3.4. Photo-oxidative stability

The photo-stability of ZnPc-loaded nanoemulsions was analyzed in water by measuring the decrease in the intensity of the Q-band over the time of irradiation with red light under air. The time decay of the absorbance maxima of the Q-band for ZnPc obeyed first-order kinetics as shown in Fig. 6.

The corresponding photodegradation constants  $k$  are listed in Table 2. Smaller values of  $k$  infer a high photo-oxidative stability. As shown in Table 2, the ZnPc incorporated into nanoemulsions showed low values of  $k$ , thus indicating that it is stable during the irradiation time of our experiments. Moreover, ZnPc-loaded NE2 presented the highest stability in water.

Table 2

Photophysical parameters and photodegradation constants  $k$  obtained for ZnPc in THF, and incorporated into NE1 and NE2.

ZnPc	$Q_{band}, \lambda_{max}$ (nm)	$\epsilon_{max}$ ( $M^{-1} cm^{-1}$ )	$\Phi_F$	$\Phi_{\Delta}$	$k$ ( $10^{-3} min^{-1}$ )
THF	680	$1.0 \times 10^5$	$0.31 \pm 0.01$	$0.66 \pm 0.01$	0.70
NE1	681	$8.9 \times 10^4$	$0.14 \pm 0.01$	$0.58 \pm 0.04$	1.62
NE2	682	$4.1 \times 10^4$	$0.12 \pm 0.02$	$0.38 \pm 0.03$	0.54

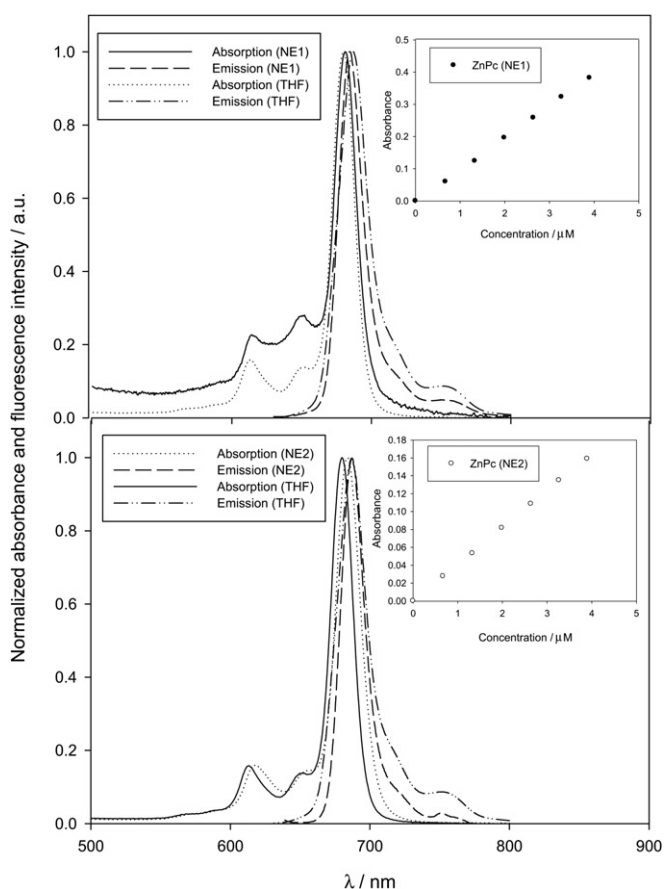
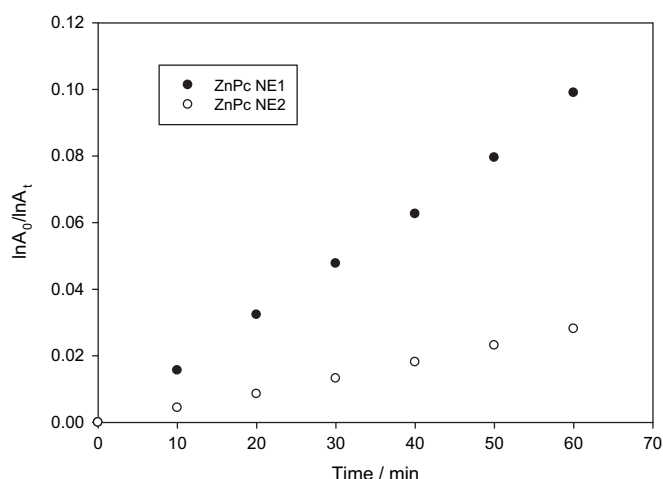


Fig. 5. Absorption and emission spectra of ZnPc in THF, and incorporated into NE1 and NE2. Inset: Lambert–Beer law verified at  $\lambda_{max}$ .



**Fig. 6.** First-order plots for the photodegradation of ZnPc incorporated into NE1 and NE2.

### 3.5. Thermodynamic stability studies

Nanoemulsions are thermodynamically stable systems that are formed at particular concentrations of oil, surfactant and water, which makes them stable and not subject to phase separation, creaming or cracking. It is the thermostability that differentiates nano- or micro-emulsions from emulsions that have kinetic stability and eventually phase-separate [11,19]. Thus, the formulations were tested for their thermodynamic stability by using centrifugation, heating–cooling cycle, and a freeze–thaw cycle. Both formulations survived the thermodynamic stability test.

## 4. Conclusions

ZnPc nanoemulsion formulations were successfully prepared by the spontaneous emulsification method. Incorporation of the lipophilic photosensitizer (ZnPc) into nanoemulsions improved dye solubilization in water, thus a two- to three-fold increase in water solubility was observed for the ZnPc incorporated into NE1 and NE2 nanoemulsions in comparison with that observed for water–DMSO (98:2).

Besides, over the irradiation times studied, the ZnPc incorporated into nanoemulsions was photo-stable. Also, both nanoemulsions NE1 and NE2 exhibited thermodynamic stability.

The photophysical parameters showed that the ZnPc incorporated into NE1 and NE2 nanoemulsions are excellent singlet oxygen generators with a high value of quantum yield of single oxygen production of 0.38 and 0.58 respectively.

The morphological evaluation confirmed the formation of nanoemulsions in the nanosize range. Taking into account that viscosity values higher than 3900 cP might not be attractive for parenteral administration in clinical trials, both nanoemulsions NE1 and NE2 are excellent formulations owing to the fact that their viscosity ranged from 30.2 to 323.9 cP respectively.

These results allow us to consider ZnPc nanoemulsion formulations as promising second-generation photosensitizers for photobiological purposes.

## Acknowledgements

This work was supported by grants from the University of Buenos Aires (X-063), the Consejo Nacional de Investigaciones

Científicas y Técnicas (CONICET, PIP 104) and the Agencia Nacional de Promoción Científica y Tecnológica (PICT 1030).

## References

- [1] Macdonald IJ, Dougherty TJ. Basic principles of photodynamic therapy. *J Porphyr Phthalocyanines* 2001;5:105–29.
- [2] Rodríguez ME, Morán F, Bonansea A, Monetti M, Fernández DA, Strassert CA, et al. A comparative study of photophysical and phototoxic properties of a new octaalkyl zinc (II) phthalocyanine incorporated in an hydrophilic polymer, in liposomes and in non ionic micelles. *Photochem Photobiol Sci* 2003;2:988–94.
- [3] Rodríguez ME, Fernández DA, Awruch J, Braslavsky S, Dicalio LE. Effect of aggregation of a cationic phthalocyanine in micelles and in the presence of human serum albumin. *J Porphyr Phthalocyanines* 2006;10:33–42.
- [4] Master AM, Rodríguez ME, Kenney ME, Oleinick NL, Gupta AS. Delivery of the photosensitizer Pc 4 in PEG–PCL micelles for in vitro PDT studies. *J Pharm Sci* 2010;99:2386–98.
- [5] Konan YN, Gurny R, Allémann E. State of the art in the delivery of photosensitizers for photodynamic therapy. *J Photochem Photobiol B Biol* 2002;66: 89–106.
- [6] van Nostrum CF. Polymeric micelles to deliver photosensitizers for photodynamic therapy. *Adv Drug Deliv Rev* 2004;56:9–16.
- [7] Derycke ASL, de Witte PAM. Liposomes for photodynamic therapy. *Adv Drug Deliv Rev* 2004;56:17–30.
- [8] Torchilin VP. Multifunctional nanocarriers. *Adv Drug Deliv Rev* 2006;58: 1532–55.
- [9] Chatterjee DK, Fong LS, Zhang Y. Nanoparticles in photodynamic therapy: an emerging paradigm. *Adv Drug Deliv Rev* 2008;60:1627–37.
- [10] Eccleston MJ. Microemulsions. In: Swarbrick J, Boylan JC, editors. *Encyclopedia of pharmaceutical technology*, vol. 9. New York: Marcel Dekker; 1994. p. 375–421.
- [11] Lawrence MJ, Rees GD. Microemulsion-based media as novel drug delivery system. *Adv Drug Deliv Rev* 2000;45:89–121.
- [12] García Vior MC, Dicalio LE, Awruch J. Synthesis and properties of phthalocyanine zinc(II) complexes replaced with oxygen and sulfur adamantane moieties. *Dyes Pigm* 2009;83:375–80.
- [13] Fernández DA, Awruch J, Dicalio LE. Photophysical and aggregation studies of *t*-butyl substituted Zn phthalocyanines. *Photochem Photobiol* 1996;63:784–92.
- [14] Bouchemal K, Briançon S, Perrier E, Fessi H. Nano-emulsion formulation using spontaneous emulsification: solvent, oil and surfactant optimisation. *Int J Pharm* 2004;280:241–51.
- [15] Glisoni RJ, Chiappetta D, Finkelsztajn LM, Moglioni AG, Sosnik A. Self-aggregation behaviour of novel thiosemicarbazone drug candidates with potential antiviral activity. *New J Chem* 2010;34:2047–58.
- [16] Wilkinson F, Herman WP, Rose AD. Rate constant for the decay and reactions of the lowest electronically excited singlet state of molecular oxygen in solution. An expanded and revised compilation. *J Phys Chem Ref Data* 1995; 24:663–1021.
- [17] Kraljic I, El Mohsni S. A new method for the detection of singlet oxygen in aqueous solutions. *Photochem Photobiol* 1978;28:577–81.
- [18] Schnurpfeil G, Sobbi AK, Spillger W, Kliesch H, Wöhrle DJ. Photo-oxidative stability and its correlation with semi-empirical MO calculations of various tetraazaporphyrin derivatives in solution. *J Porphyr Phthalocyanines* 1997;1: 159–67.
- [19] Shafiq S, Shakeel F, Talegaonkar S, Ahmad FJ, Khar RK, Ali M. Development and bioavailability assessment of ramipril nanoemulsion formulation. *Eur J Pharm Biopharm* 2007;66:227–43.
- [20] Pouton CW. Formulation of poorly water-soluble drugs for oral administration: physicochemical and physiological issues and the lipid formulation classification system. *Eur J Pharm Sci* 2006;29:278–87.
- [21] Kale A, Patravale V. Development and evaluation of lorazepam micro-emulsions for parenteral delivery. *AAPS PharmSciTech* 2008;9:966–71.
- [22] Palamakula A, Khan MA. Evaluation of cytotoxicity oils used in coenzyme Q<sub>10</sub> Self-emulsifying Drug Delivery System (SEDDS). *Int J Pharm* 2004;273:63–73.
- [23] Porter CJH, Pouton CW, Cuine JF, Charman WN. Enhancing intestinal drug solubilization using lipid-based delivery systems. *Adv Drug Deliv Rev* 2008; 60:673–91.
- [24] Tagne JB, Kakumanu S, Ortiz D, Shea T, Nicolosi R. A nanoemulsion formulation of tamoxifen increases its efficacy in a breast cancer cell line. *J Mol Pharm* 2008;5:280–6.
- [25] Charman SA, Charman WN, Rogge MC, Wilson TD, Dutko FJ, Pouton CW. Self-emulsifying drug delivery systems: formulation and biopharmaceutical evaluation of an investigational lipophilic compound. *Pharm Res* 1992;9: 87–93.
- [26] Tall B, Yalkowski SH. Enhanced intestinal absorption of cyclosporine in rats through the reduction of emulsion droplet size. *Pharm Res* 1989;6:40–3.
- [27] Boonme P, Krauel K, Graf A, Rades T, Junyaprasert VB. Characterization of microemulsion structures in the pseudoternary phase diagram of isopropyl palmitate/water/Brij 97:1-butanol. *AAPS PharmSciTech* 2006;7:45.
- [28] Weiwei Z, Aihua Y, Weihong W, Ruiqian D, Jun W, Guangxi Z. Formulation design of microemulsion for dermal delivery of penciclovir. *Int J Pharm* 2006; 360:184–90.

- [29] Rumie Vittar NB, Prucca CG, Strassert C, Awruch J, Rivarola VA. Cellular inactivation and antitumor efficacy of a new zinc phthalocyanine with potential use in photodynamic therapy. *Int J Biochem Cell Biol* 2008;40:2192–205.
- [30] Strassert CA, Bilmes G, Awruch J, Dixelio LE. Comparative photophysical investigation of oxygen and sulfur as covalent linkers on octalylamino substituted zinc(II) phthalocyanine. *Photochem Photobiol Sci* 2008;7:738–47.
- [31] Minnes R, Weitman H, You Y, Detty MR, Ehrenberg B. Dithiaporphyrin derivatives as photosensitizers in membranes and cells. *J Phys Chem B* 2008;112:3268–76.
- [32] Diz VE, Gauna GA, Strassert CA, Awruch J, Dixelio LE. Photophysical properties of microencapsulated photosensitizers. *J Porphyr Phthalocyanines* 2010;14:278–83.